Identification of nonlinear Anti-vibration isolator properties

Fares MEZGHANI [1,2], Alfonso Fernández DEL RINCÓN [2], Mohamed Amine BEN SOUF [1], Pablo García FERNANDEZ [2], Fakher CHAARI [1,*], Fernando Viadero RUEDA [2], Mohamed HADDAR [1]

[1] *Laboratory of Mechanics, Modelling and Production, National school of Engineering of Sfax, University of Sfax, Sfax, Tunisia*

[2] *Laboratory of Structural and Mechanical Engineering, Superior Technical School of Industrial Engineering and Telecommunications, University of Cantabria, Santander, Spain*

Abstract

Vibrations are classified among the major problems of the engineering structures. Anti-Vibration isolators are used to absorb vibrational energy and minimize forces causing damage. The isolator is modelled as a parallel combination of stiffness and damping elements. The main purpose of the model is to enable designers to predict a dynamic system response under different structural excitations and boundary conditions. A method of nonlinear identification, discussed in this paper, aims to provide a tool for engineers to extract information about nonlinear dynamic behaviour using measured data from experiments. The proposed method is demonstrated and validated with numerical simulations. Thus, an application of this technique for identifies the nonlinear parameters is illustrated. Nonlinear stiffness and nonlinear damping can decrease with the increase of amplitude of the base excitation. The softening behaviour of the mesh isolator is clearly visible.

Keywords: Anti-vibration isolator, dynamic behaviour, transmissibility measured data, numerical simulations.

*Corresponding author. E-mail address: fakher.chaari@gmail.com

December 23, 2016

1. introduction

In many engineering applications, it is required to minimize the transfer of vibrations from the source to receiver. In order to solve this problem and reduce the transmitted vibration, a vibration isolator should be added. From several isolation techniques, the passive isolator has been widely applied in engineering due to its simple design and high reliability. Different kinds of passive isolators are applied in many fields. For instance, typical vibration isolators employ metal coil spring to store the energy due to resilience and to maintain the force between contacting surfaces. Elastomeric shock mounts, such as rubber isolators which absorb mechanical energy by deforming, play an important role in the noise and vibration control. They are widely used in automotive engines [1], aircraft components, industrial machinery and building foundations. In practice, air spring, pneumatic and elastomeric vibration mount, are also commonly used as an important fundamental part of mechanical equipment requiring low natural frequency isolation and automobile suspension system [2]. Viscoelastic material isolators are considered as a relatively new damping material and have been extensively used in aerospace applications [3]. There are various types of this kind [4, 5, 6]: such as the vibration isolator using Solid-And- Liquid-Mixture (SALiM) [7] which was inspired by Yamamoto [8]. Further to that, Courtney carried out some experiments on shock absorbing liquid absorber to validate its basic properties, and referred to SALiM liquid [9, 10]. Another kind of passive isolators is the passive negative stiffness isolator [11, 12] which is a revolutionary concept in low-frequency vibration isolation. This isolator is provided by a spring that supports a load, combined with two springs, which are called corrector or auxiliary springs, act as negative stiffness mechanism. The metal mesh isolator, which is essentially stainless steel wires crimped, rolled or compressed into any geometric shape that is required, is one of the important passive vibration isolation products Stop-Shock. It can provide a solution for many engineering applications, for example, engines and gearboxes supports, railway lines, suspension bump stops. Since, it not only has higher stiffness than the elastomeric materials, but also offers larger hysteresis loops and provides excellent isolation performance [13].

In order to design a nonlinear system, a nonlinear modal analysis, based on mathematical models of a single-degree-of-freedom system, is carried out. The modal quantities depend on several variables: amplitude of vibration, frequency of excitation, stiffness and damping parameters. The main pur-

pose to use nonlinear modal analysis methods is to allow engineers to identify and quantify the nonlinearity in a standard testing environment. The most significant application of modal testing is to compare the numerical analysis with experimental data and to apply the necessary changes on the model, in order to obtain satisfactory results.

The identification and quantification of nonlinearity has drawn much attention. There are available many currently available techniques, presented in [14, 15]. Worden and Tomlison [16] summarized the background of harmonic balance method and the Hilbert transform. The latter was used by Feldman, M. to propose a method that studies the dynamic system for: free vibration analysis "FREEVIB" [17] and forced vibration analysis "FORCEVIB" [18]. Kershen et al. [19] classified the identification methods according to seven categories. Some cited methods are: the Restoring Force Surface (RFS) [20], the Inverse Method [21] and the Linearity Plots [22]. The RFS works in the time domain and the starting point is the application of the Newton's second law. Moreover, Rice, H.J. [23] identified the nonlinear parameters using equivalent linearization and determined the optimum one by minimizing the average of the least square of the error. Guo [24] evaluated the transmissibility of nonlinear viscously damped vibration system under harmonic excitation using a new method, based on the Ritz-Galerkin method, to investigate the effect of the damping characterization parameters on this system. A. Carrella [25, 26, 27] has recently presented a new approach, Code for Nonlinear Characterisation from mEasured Response To VibratiOn, to identify and quantify the dynamic behaviour of vibration isolators, based on the analysis of experimental data. CONCERTO is applied to a single-degree-of-freedom (SDOF) system which is subjected to harmonic base excitation or harmonic force excitation. The principle, upon which the approach is based, is effectively a linearization; at given response amplitude, the stiffness and the damping are considered constant. It is also assumed that the system responds at the same frequency as the excitation.

The newness of this work is the employment of the identification method mentioned previously to reconstruct the nonlinear stiffness and damping functions of a metal mesh isolator. This article aims at investigating the dynamic properties of the examined isolator under different levels of excitation in order to improve the reduction of transmitted vibrations. This paper is organised as follows: the following Section introduces the procedure proposed in this work; in the third section, a comparison is performed with an existing nonlinear identification method based on measured transmissibility

[27] in order to validate the numerical model qualitatively and quantitatively; the transmissibility measured data are analyzed to characterize and identify the nonlinear stiffness and damping of the investigated isolator in the fourth Section.

2. Theoretical study

In this section, a methodology is presented and discussed. It consists of the measurement of the transmissibility (displacement) from appropriate responses, in one hand and on extracting frequency (stiffness) and damping functions, in the other hand.

2.1. Overview of CONCERTO: Code for Nonlinear Characterisation from mEasured Response To VibratiOn:

The CONCERTO, presented in [25, 26, 27], is a frequency-domain method, whose its aims is the identification and quantification of nonlinear parameters [25] from measured FRF [26] and transmissibility data [27]. This method is used to analyse numerical and experimental data [27].

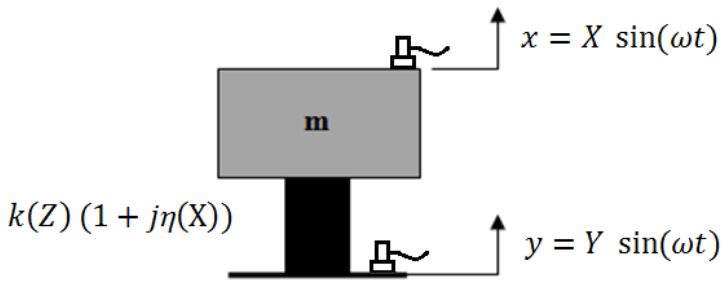

Figure 1: SDOF system of a suspended mass on a nonlinear mount with complex stiffness and under base excitation

The proposed SDOF identification method, based on the assumption that the studied system with nonlinear stiffness and damping subjected to harmonic base excitation, can be depicted through the equation of motion as follows:

$$m\ddot{z} + k(1 + j\eta)z = m\omega^2 Y \sin(\omega t) \tag{1}$$

where $z = x - y$ represents the deformation of the mount, ω the excitation frequency, k and η are the stiffness and damping loss factor respectively. The absolute transmissibility is defined as the non-dimensional quantity that tells how the motion is transmitted from the base to the mass at various frequencies. It is measured as the ratio between the output and the input displacements.

$$|T| = |\frac{X}{Y}| = |\frac{k(1+j\eta)}{k(1+j\eta) - m\omega^2}| \tag{2}$$

This can be rewritten in terms of modal quantities as:

$$|T| = |\frac{X}{Y}| = |\frac{\omega_0^2 + j\omega_0^2\eta}{\omega_0^2 - \omega^2 + j\omega_0^2\eta}| \tag{3}$$

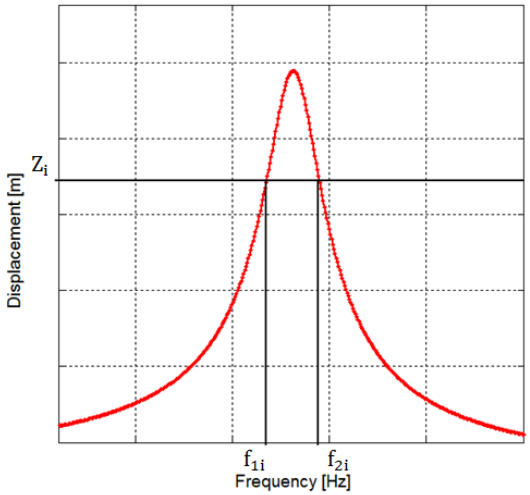

Figure 2: linearisation process of CONCERTO

For given amplitude Z_i, there is a pair of frequencies points (see Fig. 2). The displacement curve Vs. frequency contains information which are required to calculate the natural frequency $\omega_0(Z_i)$ and the loss factor $\eta(Z_i)$ at that particular amplitude as:

$$\omega_0^2(Z_i) = \frac{(R_{2i} - R_{1i})(R_{2i}\omega_{2i}^2 - R_{1i}\omega_{1i}^2) + (I_{2i} - I_{1i})(I_{2i}\omega_{2i}^2 - I_{1i}\omega_{1i}^2)}{(R_{2i} - R_{1i})^2 + (I_{2i} - I_{1i})^2} \tag{4}$$

$$\eta(Z_i) = |\frac{-(I_{2i} - I_{1i})(R_{2i}\omega_{2i}^2 - R_{1i}\omega_{1i}^2) + (R_{2i} - R_{1i})(I_2 i\omega_{2i}^2 - I_{1i}\omega_{1i}^2)}{\omega_r^2(Z_i)((R_{2i} - R_{1i})^2 + (I_{2i} - I_{1i})^2)}| \quad (5)$$

where R_1 and R_2 (I_1 and I_2) are the real (imaginary) parts of the transmissibility at the amplitude Z_i, that have been measured at the frequencies ω_1 and ω_2, before and after the resonance peak, respectively.

In order to quantify the nonlinear parameters, it is necessary to evaluate the stiffness and damping functions, from the functions of natural frequency and loss factor.

Once the model mass, presenting the mass of the system divided by the number of mounts in the system, has been determined, the stiffness function $k(Z_i)$ can thus be obtained by multiplying the mass by the natural frequency expressed in Eq.(4).

$$k(Z_i) = \omega_0^2(Z_i)m \quad (6)$$

In addition, the damping function $C(Z_i)$ can be extracted using the relationship [25]:

$$C(Z_i) = \eta(Z_i)\omega_0(Z_i)m \quad (7)$$

2.2. Analytical stiffness and damping functions using Harmonic Balance

In order to evaluate the efficiency of the method, analytical expressions for the stiffness and damping functions have been derived using the Harmonic Balance Method to solve the nonlinear differential equations [16].

In fact, the effective expressions correspond to the stiffness and damping of a linearised system under the assumption that the system responds at the same frequency as the harmonic excitation. This is equivalent to the analytical expressions determined by applying the first-order expansion of the Harmonic Balance approximation in the steady state.

The dynamic equation describing the motion of a SDOF system, subjected to a harmonic excitation, could be written as:

$$m\ddot{z} + f_d(\dot{z}) + f_s(z) = y(t) \quad (8)$$

where z and y denote the response and the excitation, respectively. $f_d(\dot{z})$ is the nonlinear damping function and $f_s(z)$ is the nonlinear stiffness function. For stable state harmonic vibration, the displacement response can be expressed as:

$$z(t) = Z\sin(\omega t) \quad (9)$$

The analysis will be simplified by considering the equation of motion as follows:

$$m\ddot{z} + C_{eq}\dot{z} + K_{eq}z = y(t) \tag{10}$$

where C_{eq} and K_{eq} present the equivalent damping and stiffness, respectively.

2.2.1. Nonlinear Stiffness

The nonlinear stiffness function can be expanded using the Fourier series, neglecting all the higher-order terms and only the fundamental term (first harmonic) is considered.
So:

$$f_s(z) \cong a_{k0} + a_{k_1}\cos(\omega t) + b_{k1}\sin(\omega t) = K_{eq}z(t) \tag{11}$$

where a_{k0}, a_{k_1} and b_{k_1} are the Fourier coefficients of the fundamental term expressed as:

$$\begin{aligned} a_{k_0} &= \frac{1}{2\pi}\int_0^{2\pi} f_s(z(t))d\theta \\ a_{k_1} &= \frac{1}{\pi}\int_0^{2\pi} f_s(z(t))\cos\theta d\theta \\ b_{k_1} &= \frac{1}{\pi}\int_0^{2\pi} f_s(z(t))\sin\theta d\theta \end{aligned} \tag{12}$$

The mathematical model of a cubic stiffness element can be expressed as:

$$f_s(z) = kz + k_{nl}z^3 \tag{13}$$

So, substituting Eq.(13) into Eq. (12), the Fourier coefficients will be calculated:

$$\begin{aligned} a_{k0} &= 0 \\ a_{k_1} &= 0 \\ b_{k_1} &= k_1 Z + \frac{3}{4}k_{nl}Z \end{aligned} \tag{14}$$

Therefore,

$$K_{eq} = k + \frac{3}{4}k_{nl}Z^2 \tag{15}$$

where k and k_{nl} represent the linear and the nonlinear stiffness parameters, respectively.

2.2.2. Nonlinear Damping

The nonlinear damping function can be rewritten as follow:

$$f_d(\dot{z}(t)) \cong a_{c0} + a_{k_1}\cos(\omega t) + b_{c1}\sin(\omega t) = C_{eq}\dot{z}(t) \tag{16}$$

where a_{c0}, a_{c_1} and b_{c_1} are the Fourier coefficient of the fundamental term.

$$\begin{aligned} a_{c_0} &= \frac{1}{2\pi}\int_0^{2\pi} f_d(\dot{z}(t))d\theta \\ a_{c_1} &= \frac{1}{\pi}\int_0^{2\pi} f_d(\dot{z}(t))\cos\theta d\theta \\ b_{c_1} &= \frac{1}{\pi}\int_0^{2\pi} f_d(\dot{z}(t))\sin\theta d\theta \end{aligned} \tag{17}$$

Combining Eq.(16) and Eq.(17) leads to:

$$C_{eq} = \frac{a_{c_1}}{\omega Z} = \frac{1}{\omega Z\pi}\int_0^{2\pi} f_d(\omega Z\cos\theta)\cos\theta d\theta \tag{18}$$

The mathematical model of a quadratic damping element can be expressed as:

$$f_d(\dot{z}) = c\dot{z} + c_{nl}\dot{z}|\dot{z}| \tag{19}$$

Then the equivalent damping is given by:

$$C_{eq} = \frac{c}{\omega Z\pi}\int_0^{2\pi} \omega Z\cos\theta\cos\theta d\theta + \frac{c_{nl}}{\omega Z\pi}\int_0^{2\pi} \omega Z\cos\theta|\omega Z\cos\theta|\cos\theta d\theta \tag{20}$$

After integration, this becomes:

$$C_{eq} = c + \frac{8}{3\pi}c_{nl}\omega Z \tag{21}$$

where ω is the natural frequency of linear system and Z is the amplitude of the response at steady state. c and c_{nl} represent the linear and the nonlinear damping parameters, respectively.

3. Numerical simulations of transmissibility data for Nonlinear systems

In this section, a set of numerical simulations of nonlinear SDOF systems are presented to illustrate the applicability of the approach discussed above. Table 1 summarises the type of nonlinearity and the numerical values used in each case. In addition, the parameters of the underlying linear system are described in Table 1. All the simulation refer to the systems which are modelled as:

$$m\ddot{z} + c\dot{z} + f_c(\dot{z}) + kz + f_k(z) = m\omega^2 Y \sin(t) \tag{22}$$

where $z = x - y$ is the relative displacement between the mass and the base and Y the amplitude of the base excitation. f_c and f_k represent the nonlinear damping and stiffness respectively.
Eq.(22) has been solved using direct integration with the Matlab solver ODE45 which is the Runge-Kutta 4^{th} and 5^{th} order method for ordinary differential equations at different frequencies of excitations. Then, the absolute displacement has been determined by computing the ratio between the Fourier coefficient of the response and the amplitude of the base excitation.

Table 1: Type and values of nonlinearities for the numerical simulation

Mass $m = 1.5kg$, Damping coefficient $c = 0.8Ns/m$, $k = 6000N/m$

Nonlinearity	Damping f_c	Stiffness f_k	*Values*
cubic stiffness + Quadratic damping	$f_c = C_{nl}\dot{z}\lvert\dot{z}\rvert$	$f_k = k_{nl}z^3$	$k_{nl} = 7e^6 Nm^{-3}$ $C_n l = 8Ns^2m^{-2}$

In order to validate the results obtained with CONCERTO approach, a comparison is performed with the nonlinear identification method based on measured transmissibility and presented in [27] and then with the analytical expressions for the stiffness functions explained in section 2.3. Figs. 3 - 4 show the results obtained to analyse the transmissibility of a system with combined nonlinearities (quadratic damping + cubic stiffness) and excited by a harmonic base oscillation with amplitude $Y = 0.4\ 10^{-3}m$ and $Y = 0.15\ 10^{-3}m$, respectively.

The information about the nonlinearities of the system is provided in the two plots: one depicts the stiffness, Eq.(6), and the other the damping, Eq.(7), as a function of the amplitude of vibration displacement response of the mass. From the stiffness and damping plots, it can be seen that by increasing the level of excitation, and thus the amplitude of response, there is an increase in stiffness and damping. This increase suggests a hardening stiffness.
From the Figs. 3(b, c) and 4(b, c), we notice that these results show a quite noticed agreement between the extracted stiffness and its analytical equivalent expression. But, errors are introduced in the estimation of damping due, perhaps, to CONCERTO's interpolation whose limitations are that the determination of the stiffness and damping values is based on points which physically do not exist but are a pure numerical artefact [26].

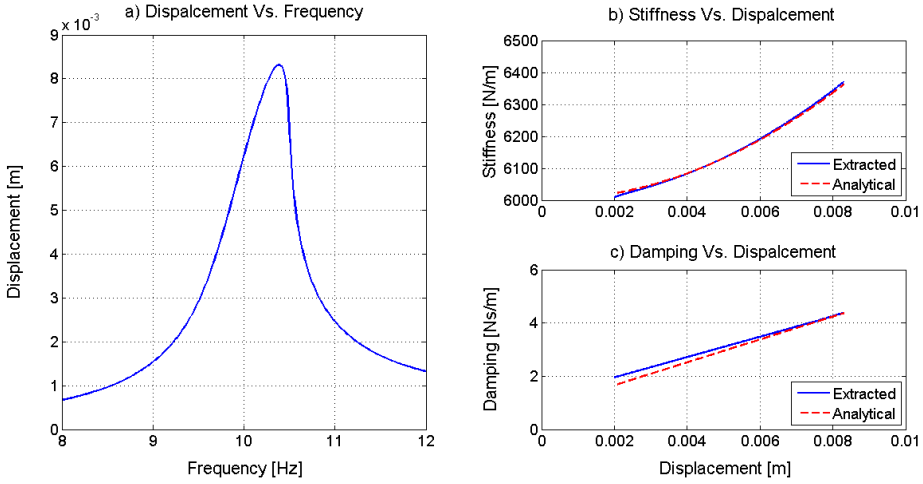

Figure 3: Numerical analysis of the system with cubic stiffness and quadratic damping excited with amplitude 0.4 10^{-3}

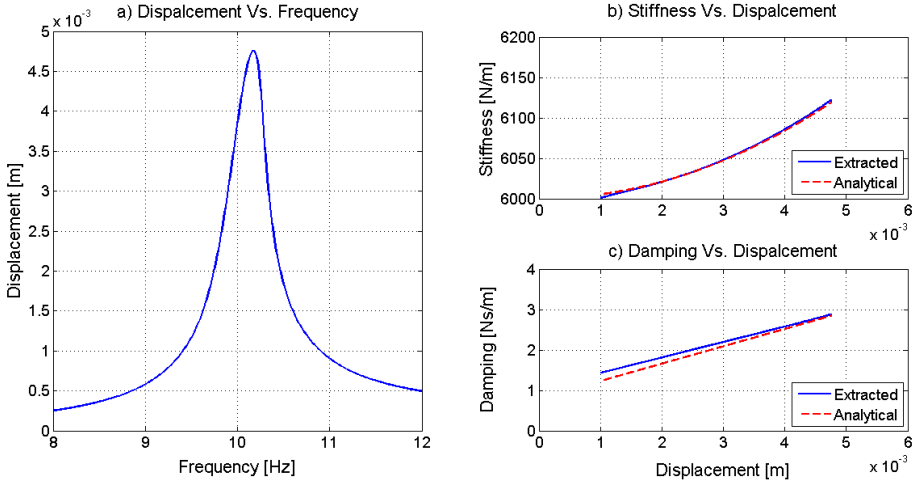

Figure 4: Numerical analysis of the system with cubic stiffness and quadratic damping excited with amplitude 0.15 10^{-3}

4. Experimental set up, results and discussions

In the following section, an experimental investigation is performed to determine the nonlinear properties of a commercially metal mesh isolator which can be inserted between the source of vibrations and the receiver. Experimental tests were designed to characterize and identify the nonlinear stiffness and damping of this isolator.

4.1. Measurement

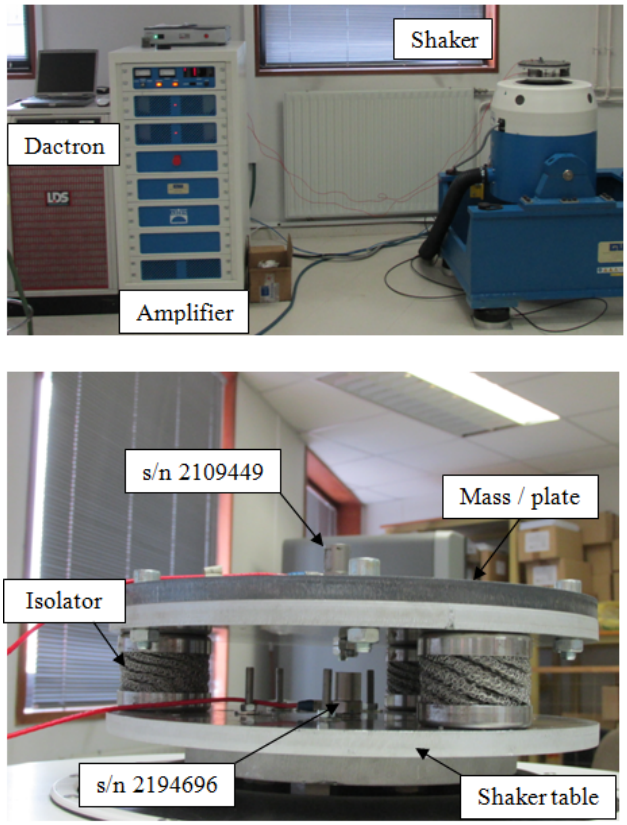

Figure 5: Test machine

The experiments are performed in an electro-dynamic shaker Gearing and Watson $V400$, connected to an amplifier $DSA4-8k$. The experimental set up is established in Fig. 5.The exciter was positioned vertically and has been controlled by a USB laser system through the Dactron associated software for data acquisition and analysis. Two accelerometers (Brüel & Kjær, type 4398) are axially placed: one on the shaker table (model s/n 2194696) and another on the mass plate (model s/n 2109449). The transmissibility could be determined by the ratio of the two signals.
In order to study the mounts behavior under different static loads, three masses were used M1, M2 and M3 which are dependent on the number of

Table 2: values and number of plates used during the test

	Number of plates	*Mass values*
$M1$	1	$5686.2g$
$M2$	4	$17552.6g$
$M3$	7	$29270.3g$

plates. The mass values used during the test are given in Table 2.

4.2. Material: the test object

Metal mesh isolators are essentially stainless steel wires; woven using knitting machine, rolled and/or pressed into the required geometric shape via a press mould. The density of the mesh isolators were determined by the knitting and pressing method. Metal mesh material can be manufactured to accommodate specific application needs including railway, engine mounts, and vibration absorbers.

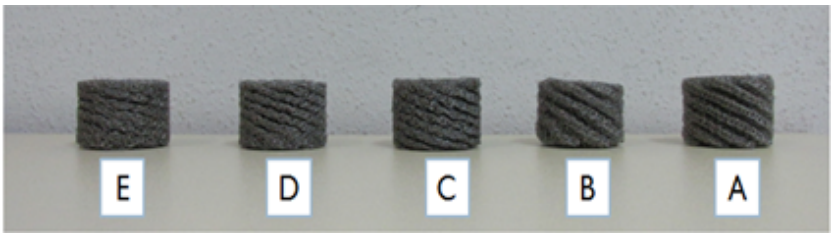

Figure 6: Five models of isolators

Five models of isolators (A, B, C, D, E), that differ in the density as shown in Fig. 6, are selected as the test element for the experimental investigation. Measurements, which have been carried out according to the method established above, aim to identify the dynamic characterization of the nonlinear isolator.

4.3. Sine sweep excitation

Three levels of acceleration ($a_1 = 1m/s^2$, $a_2 = 2m/s^2$ and $a_3 = 3m/s^2$), for each mass and isolator, have been used for exciting the structure with

the stepped-sine signal starting at $5Hz$ and increasing with a constant frequency step to a maximum frequency of $50Hz$. At each excited frequency, the transmissibility was detected using the ratio of the vibration amplitude being measured in the system to the vibration amplitude entering the system. Tests were performed for each of aforementioned cases.

(a) Acceleration response

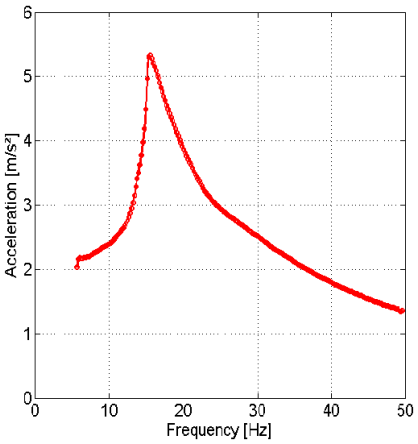

(b) Transmissibility response

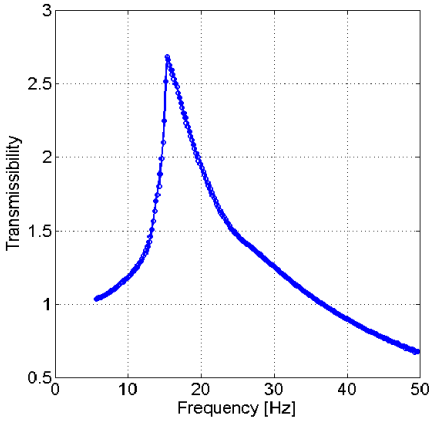

Figure 7: Sine sweep test; Model A, Mass 1, Acceleration 3

Fig.s 7(a, b) present the results of the sine sweep of the isolator model A, obtained with M1 and excited by the second level of acceleration ($a_2 = 2m/s^2$), which is kept constant during the test. Fig. 6(a) depicts the acceleration response measured by the output accelerometer of the mass. Fig. 6(b) shows the transmissibility, which was computed as the ratio of the mass acceleration measured by the accelerometer s/n 2194696, and the base acceleration measured by the accelerometer s/n 2109449, as indicated in Fig. 4.1.

It is observed that the peak on the curve, at around $15Hz$, is representative of that isolator's resonance frequency. It can be also noticed that the vibration isolation occurs when the curve crosses the transmissibility-axis into one, i.e. for frequencies above $36.5Hz$.

Fig. 8(a, b) show the results of the transmissibility response of the isolators A and B using $M2$ and for the three level of acceleration inputs. From Figs. 7(a) and 7(b), it can be seen that by increasing the level of the acceleration, the resonance frequency of the system decreases and the amplitude increases,

as well, the transmissibility decreases at high frequencies.
Otherwise, the higher level of excitation, the lower is the damping and the stiffness of the isolator and the earlier is the vibration isolation region. The deviation, lean of the curve towards lower frequencies, is a result of the softening behaviour.

(a) Model A (b) Model B

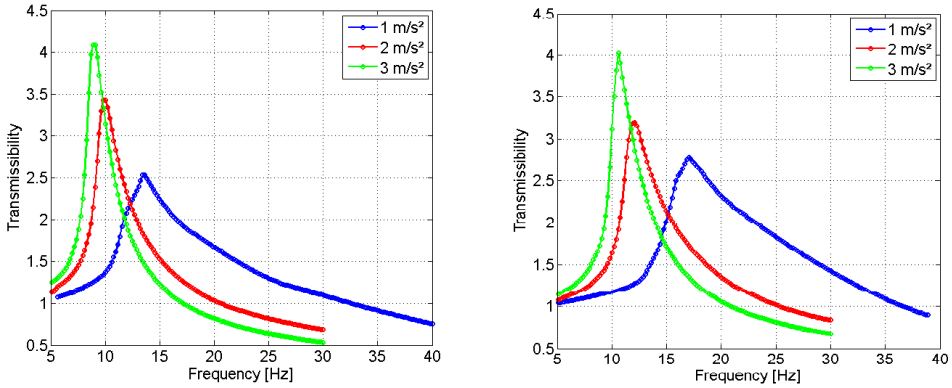

Figure 8: Sine sweep test; Mass 2

The curves of transmissibility of the both isolators B and C measured for the second level of acceleration ($a_2 = 2m/s^2$) and using the three masses (M_1,M_2 and M_3) are shown in Fig. 9(a, b). It is noteworthy that, as the weight of preload increases, the resonance frequency decreases and the frequency, at which the transmissibility is less than one, decreases; from $43Hz$ for M_1 (Fig. 8(a)) to $22.5Hz$ for $M3$. This is because the compressing of the isolator dominated the contributions to the value of stiffness and the stiffness dominated the response at low frequencies.

(a) Model B (b) Model C

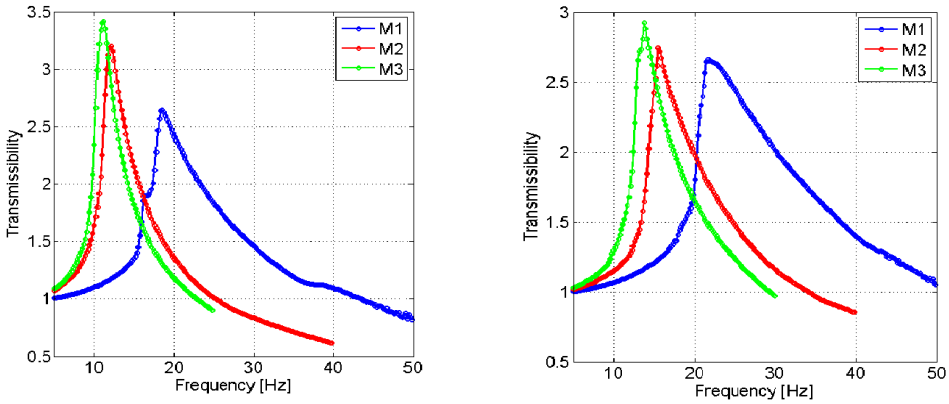

Figure 9: Sine sweep test; Acceleration 2

The transmissibility results of the five isolators are compared in Fig. 10. This comparison was done for the third level of acceleration and using the third mass M_3. From model A to model E, the resonance frequency increases and the amplitude decreases. In addition, the frequency at which the mount begins to isolator the vibration. This means that, the higher the density of the isolator, the larger the isolation frequency bandwidth.

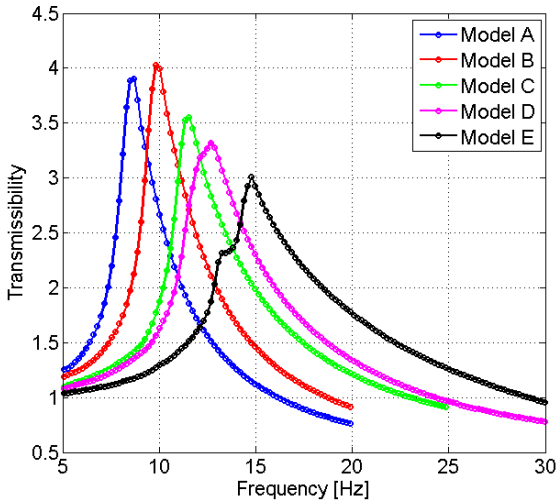

Figure 10: Sine sweep test; Mass 3, Acceleration 3

Now, a vibration test was conducted with both increasing and decreasing frequency. Experiments were performed using isolator model C, under M3 and for levels of acceleration of $2m/s^2$ and $3m/s^2$. The graphs of the run up sweep and run down sweep are shown in Fig. 11(a, b); the down sweep peak shifts away from the up sweep peak. It is notably that the hysteresis and the jump phenomenon have been observed [28]. These are the characteristic of the softening behavior of the metal mesh isolator.

(a) $2m/s^2$ (b) $3m/s^2$

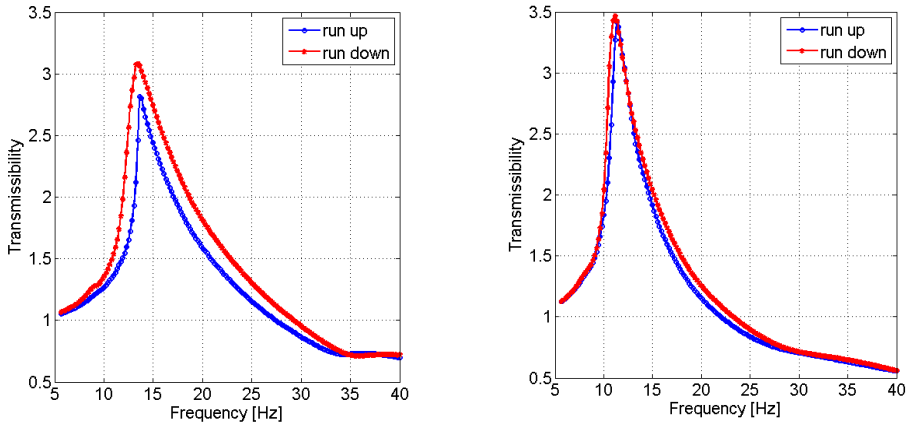

Figure 11: Sine sweep test; Model C, Mass 3

4.4. Nonlinear modelling

4.4.1. Application of the method

The transmissibilities measured for the three level of excitation have been analysed with CONCERTO approach which was established in section 2 and validated in Section 3. For sake of space, only the results obtained with $M2$ will be presented.

Figs. $12 - 16$ show the variation of natural frequency and damping as function of displacement. The data shown in these figures. have been normalised. The normalisation ratio of the Stiffness and Damping against the amplitude of vibration displacement is consistent rather than random.

(a) Normalised Stiffness Vs. Normalised Displacement

(b) Normalised Damping Vs. Normalised Displacement

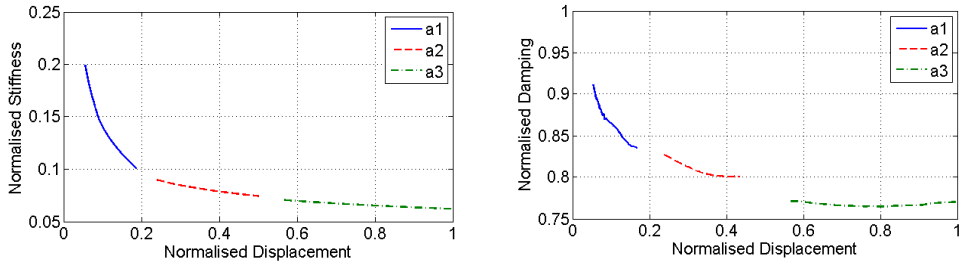

Figure 12: Extracted stiffness and damping from experimental data; Model A, Mass 2

(a) Normalised Stiffness Vs. Normalised Displacement

(b) Normalised Damping Vs. Normalised Displacement

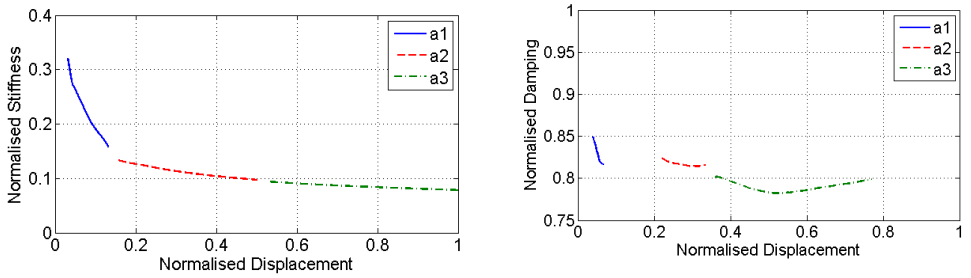

Figure 13: Extracted stiffness and damping from experimental data; Model B, Mass 2

(a) Normalised Stiffness Vs. Normalised Displacement

(b) Normalised Damping Vs. Normalised Displacement

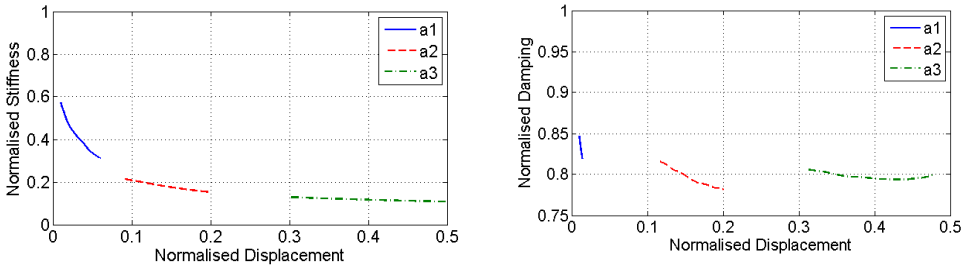

Figure 14: Extracted stiffness and damping from experimental data; Model C, Mass 2

(a) Normalised Stiffness Vs. Normalised Displacement

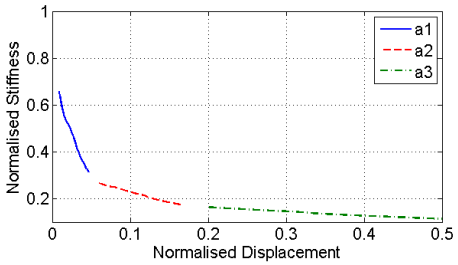

(b) Normalised Damping Vs. Normalised Displacement

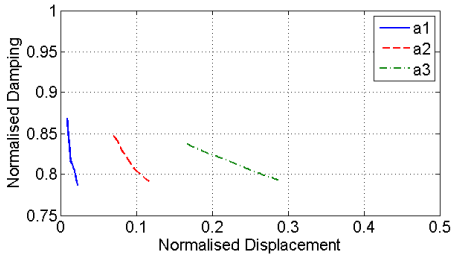

Figure 15: Extracted stiffness and damping from experimental data; Model D, Mass 2

(a) Normalised Stiffness Vs. Normalised Displacement

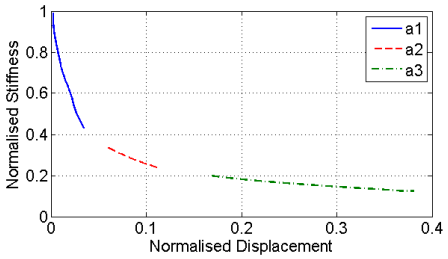

(b) Normalised Damping Vs. Normalised Displacement

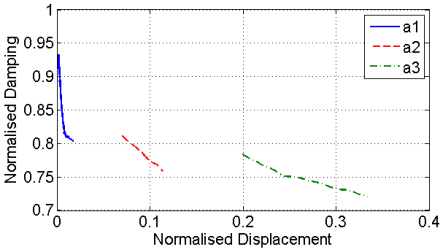

Figure 16: Extracted stiffness and damping from experimental data; Model E, Mass 2

These Figs. show that the stiffness and the damping decrease with the increasing of the displacement. As the level of excitation increases, the response displacement increases too while the values of stiffness and damping decrease. What is remarkable is that, the softening type nonlinearity of the mesh isolator is clearly visible, similar to what was shown in section 4.3. On the other hand, we notice that, from isolator A to isolator E, the stiffness increases. This fact is due to the manufacturing and knit method of each isolator.

4.4.2. Identification of the nonlinear parameters of the isolator

The MATLAB basic fitting approach is applied to the curves extracted from CONCERTO, shown in Figs. 12 − 16, to determine the function of the

Stiffness and Damping. The functions of fitted curve stiffness and damping from the curve fitting are as follows:

$$K_{fitted} = \alpha_1 + \alpha_2 Z + \alpha_3 Z^2 \tag{23}$$

$$C_{fitted} = \mu_1 + \mu_3 Z^2 \tag{24}$$

where (α_1,α_2,α_3) and (μ_1,μ_3) are the coefficients determined from MATLAB basic fitting.

Combining the equations (23) - (24) and the equivalent stiffness (Eq. (25)) and damping (Eq.(26)) functions proposed by [29], the nonlinear stiffness coefficients (k_1, k_2, k_3) and the nonlinear damping coefficients (c_1, c_3) of the isolator can be identified.

$$K_{eq} = k_1 + \frac{8}{3\pi} k_2 Z + \frac{3}{4} k_3 Z^2 \tag{25}$$

$$C_{eq} = c_1 + \frac{3}{4} \omega^2 c_3 Z^2 \tag{26}$$

As an example, the measured transmissibility curve of the isolator type A, obtained with $M2$ excited by the second acceleration ($a_2 = 2m/s^2$) is plotted as blue line in Fig. 17. In the same figure, the numerical solution using direct integration using $ODE45$ is shown for comparison.

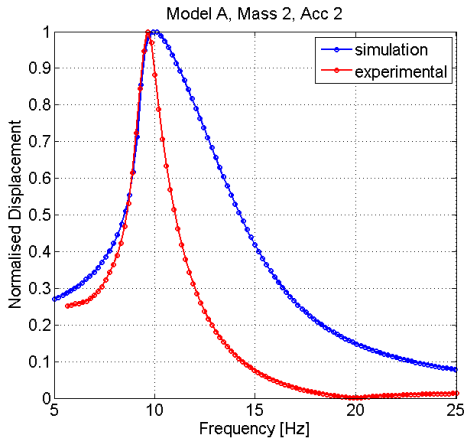

Figure 17: Comparison between numerical simulation and measured data; Model A, Mass 3, Acceleration 2 m/s^2

Fig. 17 indicates the good agreement between simulations and experimental in the first branch (before peak). Otherwise, the most important particularity is the adjacency in the resonant frequency and the amplitude of the resonance is almost closely. These prove the validity of the method assumption to identify the dynamic characteristic of the isolator from measured data, as mentioned in [27]. The shift between curves in the second branch (after peak) is similar to results as showing in [27]. The shift might be related to the identified coefficients of damping that has been implemented in the model (defined in Eq. (21)).The function of damping, defined in [30], that the damping force is a combination of coulomb damping, quadratic damping and viscous damping, could be implemented in the model to achieve a good coherence.

5. Conclusion

Nonlinearities in structural dynamics are common in real structures. The identification of nonlinearity parameters from experimental data is an important step to obtain a reliable and precise numerical model which will ensure a better understanding of their dynamical behaviour. This paper reviews the state of the art of the theory of vibration isolation and presents several types of nonlinear isolators. Thus, Different methods of identification are presented. One of them is investigated in order to characterise the dynamic behaviour of a SDOF system. This approach consists of realizing several steps: firstly, this method is compared with an existent identification method to validate it; then, a practical application to anti vibration isolator is presented and the linear and nonlinear parameters are extracted to be used for building a theoretical model which is used for numerical simulation. The agreement between the simulated and measured results is acceptable. But, errors are introduced in the estimation of damping due. The cause of these errors has not been fully understood and it can be speculated that this is the jump phenomenon effect. Most importantly, future works will focus on three different aspects: for instance, further exploration will be done to identify the limitations in order to improve the method presented; in addition, these works will investigate the influence of the temperature in the behaviour of the nonlinear isolator; moreover, future research should also consider the identification issues arising from the dynamic driving point stiffness using impact test.

References

[1] Z. M. Ripin, O. L. Ean, Dynamic characterization of engine mount at different orientation using sine swept frequency test, in: Regional conference on mechanical and aerospace technology, 2010, pp. 1–6.

[2] P. Polach, M. Hajžman, Design of characteristics of air-pressure-controlled hydraulic shock absorbers in an intercity bus, Multibody System Dynamics 19 (1-2) (2008) 73–90.

[3] R. Ibrahim, Recent advances in nonlinear passive vibration isolators, Journal of sound and vibration 314 (3) (2008) 371–452.

[4] C. Yilmaz, N. Kikuchi, Analysis and design of passive band-stop filter-type vibration isolators for low-frequency applications, Journal of Sound and Vibration 291 (3) (2006) 1004–1028.

[5] J. Winterflood, D. G. Blair, B. Slagmolen, High performance vibration isolation using springs in euler column buckling mode, Physics Letters A 300 (2) (2002) 122–130.

[6] N. Du Plooy, P. Heyns, M. Brennan, The development of a tunable vibration absorbing isolator, International journal of mechanical sciences 47 (7) (2005) 983–997.

[7] X. Gao, Q. Chen, H. Teng, Modelling and dynamic properties of a novel solid and liquid mixture vibration isolator, Journal of Sound and Vibration 331 (16) (2012) 3695–3709.

[8] M. Yamamoto, Compression spring, Japan, Japanese Patent (1992) 04–370427.

[9] W. A. Courtney, Preliminary investigations into the mechanical properties and potential applications of a novel shock absorbing liquid, University of Manchester, 1998.

[10] W. Courtney, S. Oyadiji, Preliminary investigations into the mechanical properties of a novel shock absorbing elastomeric composite, Journal of Materials Processing Technology 119 (1) (2001) 379–386.

[11] D. L. Platus, Negative-stiffness-mechanism vibration isolation systems, in: San Jose-DL tentative, International Society for Optics and Photonics, 1992, pp. 44–54.

[12] A. Carrella, M. Brennan, T. Waters, V. Lopes, Force and displacement transmissibility of a nonlinear isolator with high-static-low-dynamic-stiffness, International Journal of Mechanical Sciences 55 (1) (2012) 22–29.

[13] S.-H. Youn, Y.-S. Jang, J.-H. Han, Development of a three-axis hybrid mesh isolator using the pseudoelasticity of a shape memory alloy, Smart Materials and Structures 20 (7) (2011) 075017.

[14] L. Jezequel, C.-H. Lamarque, Analysis of non-linear dynamical systems by the normal form theory, Journal of sound and vibration 149 (3) (1991) 429–459.

[15] R. Lin, Identification of the dynamic characteristics of nonlinear structures, Diss. University of London.

[16] K. Worden, G. R. Tomlinson, Nonlinearity in structural dynamics: detection, identification and modelling, CRC Press, 2000.

[17] M. Feldman, Non-linear system vibration analysis using hilbert transform–i. free vibration analysis method'freevib', Mechanical systems and signal processing 8 (2) (1994) 119–127.

[18] M. Feldman, Non-linear system vibration analysis using hilbert transform–ii. forced vibration analysis method'forcevib', Mechanical Systems and Signal Processing 8 (3) (1994) 309–318.

[19] G. Kerschen, K. Worden, A. F. Vakakis, J.-C. Golinval, Past, present and future of nonlinear system identification in structural dynamics, Mechanical systems and signal processing 20 (3) (2006) 505–592.

[20] S. Masri, T. Caughey, A nonparametric identification technique for nonlinear dynamic problems, Journal of Applied Mechanics 46 (2) (1979) 433–447.

[21] J. He, D. Ewins, A simple method of interpretation for the modal analysis of nonlinear systems, in: International Modal Analysis Conference, 5 th, London, England, 1987, pp. 626–634.

[22] D. Göge, M. Sinapius, U. Füllekrug, M. Link, Detection and description of non-linear phenomena in experimental modal analysis via linearity plots, International Journal of Non-Linear Mechanics 40 (1) (2005) 27–48.

[23] H. Rice, Identification of weakly non-linear systems using equivalent linearization, Journal of Sound and Vibration 185 (3) (1995) 473–481.

[24] P. Guo, Damping system designs using nonlinear frequency analysis approach.

[25] A. Cappellini, A. Carrella, M. Feldman, Measuring dynamic nonlinearities using the frequency response and the hilbert transform methods, in: PROCEEDINGS OF ISMA2010 INCLUDING USD2010, 2010, pp. 3087–3097.

[26] A. Carrella, D. Ewins, Identifying and quantifying structural nonlinearities in engineering applications from measured frequency response functions, Mechanical Systems and Signal Processing 25 (3) (2011) 1011–1027.

[27] A. Carrella, Nonlinear identifications using transmissibility: Dynamic characterisation of anti vibration mounts (avms) with standard approach and nonlinear analysis, International Journal of Mechanical Sciences 63 (1) (2012) 74–85.

[28] M. Amabili, M. Pellegrini, M. Tommesani, Experiments on large-amplitude vibrations of a circular cylindrical panel, Journal of sound and vibration 260 (3) (2003) 537–547.

[29] G. Wang, G. Zheng, Vibration of two beams connected by nonlinear isolators: analytical and experimental study, Nonlinear Dynamics 62 (3) (2010) 507–519.

[30] Z. Hu, G. Zheng, A combined dynamic analysis method for geometrically nonlinear vibration isolators with elastic rings, Mechanical Systems and Signal Processing 76 (2016) 634–648.